NASA-CR-193433

HUGHES

HUGHES DANBURY OPTICAL SYSTEMS, INC.
a subsidiary

PR D15-0018

IN-74-CR

35P

FINAL REPORT

IMPACT OF SHORTER WAVELENGTHS ON OPTICAL QUALITY FOR LAWS

Submitted to

National Aeronautics and Space Administration
George C. Marshall Space Flight Center
Marshall Space Flight Center, AL 35812

Under Contract H-20752D

SEPTEMBER 1993

Contributors:
Robert J. Noll
James G. Tsacoyeanes
Jeanette R. Tausanovitch

HUGHES DANBURY OPTICAL SYSTEMS, INC.
100 WOOSTER HEIGHTS ROAD
DANBURY, CT 06810-7589

(NASA-CR-193433) IMPACT OF SHORTER WAVELENGTHS ON OPTICAL QUALITY FOR LAWS Final Report (Hughes Danbury Optical Systems) 35 p

N94-14473

Unclas

G3/74 0186046

HUGHES

HUGHES DANBURY OPTICAL SYSTEMS, INC.
a subsidiary

PR D15-0018

FINAL REPORT
IMPACT OF SHORTER WAVELENGTHS ON OPTICAL QUALITY FOR LAWS

Submitted to

National Aeronautics and Space Administration
George C. Marshall Space Flight Center
Marshall Space Flight Center, AL 35812

Under Contract H-20752D

SEPTEMBER 1993

HUGHES DANBURY OPTICAL SYSTEMS, INC.
100 WOOSTER HEIGHTS ROAD
DANBURY, CT 06810-7589

HUGHES

Hughes Danbury Optical Systems, Inc.
a subsidiary

Project Report No.: PR D15-0018

Title: Final Report, Impact of Shorter Wavelengths on Optical Quality for LAWS

Prepared by: *Alan B. Wissinger* — *9/30/93*
A. Wissinger, Program Manager — Date

Approved by: *George W Bossers* — *10/1/93*
George Bossers, Director
Advanced Development Lab — Date

REVISION RECORD:

Revision	Date	Affected Pages
Release	September 30, 1993	i-iii, 1 - 32

PRECEDING PAGE BLANK NOT FILMED

Introduction

Statement of the Problem

The effect of changing the laser wavelength (e.g. changing from a CO_2 laser to a solid-state laser) imposes presently unknown requirements on the laser atmospheric wind sounder (LAWS) optics and its pointing subsystem. The purpose of this research study is to explore parametrically the effects of several common aberrations (defocus, astigmatism, wavefront tilts, etc.), using the same merit function as used in the previous LAWS Phase 2 study[1].

When we started this study, we intended to investigate a reduced aperture telescope for possible use on the Quick-LAWS program. The telescope was to be afocal, have an aperture of 60 cm with an exit pupil diameter (i.e. the diameter of the transmit laser beam) the same as the baseline (1.5 m) telescope, which was ~50mm (beam expansion ratio of 12:1). The remaining optics was to be the same as in the LAWS baseline design (CO_2 laser, 9.11 micrometer wavelength), except as required to scale to the changed aperture. The laser characteristics, aperture diameter, telescope primary mirror focal ratio and other optical parameters were to be held constant. Only the laser wavelength was to be parametrically varied.

After progressing for several weeks with this plan, we learned that the diameter of a solid-state laser operating at 1-2μmeter range is typically only 10mm in diameter rather than the 50mm CO_2 laser beam diameter. The beam expansion ratio of the solid state laser system would have to be 60:1 rather than the 12:1 of a CO_2 laser system. A 60:1 expansion ratio is impractical because of the severe alignment tolerances it would require. Since the beam expansion ratio has a profound effect on the optical performance of any system, the approach was revised to incorporate an optical design that would reasonably accommodate a solid state laser having an output beam of 10mm.

We have accomplished the necessary optical design work, and the new optical design is summarized in this report.

The new design was used for the investigation of the effects of the shorter wavelengths of a solid-state laser. However, the parametric curves for the scaled-down LAWS baseline system (f/1 primary mirror) are included in an appendix for reference.

---

[1]GE AstroSpace LAWS Final Study Report, Phase 2, Contract No. NAS8-37589, June 1992.

Approach

Our analysis approach consists of three phases: optical design and sensitivity analysis, heterodyne performance prediction, and finally, allocation of optical tolerances within an error budget. The analysis tools used for each of the phases are the HDOS optical design and analysis code MEXP for the first phase, the recently developed Beam Propagation Analysis of Coherent Lidar Optics, and finally, a set of integrated spread sheet programs for the error budgets and tolerance allocation originally developed for the LAWS program by A. B. Wissinger

The centerpiece of this investigation is the copyrighted analysis and computer program (RJN-0108) written by Dr. Robert J. Noll of Hughes Danbury Optical Systems, Inc. The analysis is based on basic principles of optical physics, and it provides a clear picture of the system issues through the use of analytic expressions rather than purely numerical codes. These expressions help to guide and check the numeric evaluations that are applicable to the systems engineering aspects of the project. The emphasis of the analysis is on the optical subsystem so that its requirements can be defined.

The computer models are based on the optical heterodyne theorem implemented in a local oscillator back propagation mode. Laser light is propagated through the transmitting telescope to a target plane. In addition, the local oscillator field distribution integrated over the detector is back propagated to the target plane. The overlap integral of the transmitted intensity and the back propagated local oscillator beam for a measure of the heterodyne efficiency of the process. The back propagated local oscillator method is a computational aid in accounting for the received scattered signal from the target. It is *not* an approximation.

As a figure of merit for performance, a system efficiency parameter has been used. This parameter is similar to the one introduced by Zhao et. al. (App.OP. 29, p 4111, 1990) and uses a back-propagated local oscillator technique for computation. Our parameter is different from the conventionally used efficiency expression in that a detector weighted local oscillator field is back propagated to the target. By detector weighted we mean the detector field is integrated over a finite sized detector. In so doing the local oscillator power which appears in the shot noise is reduced somewhat from the total LO power due to the clipping of the finite sized detector. Also only the LO field inside the defined detector region is back propagated to the target.

In the equations we developed, numerical subscripts were used to denote the various planes in the system. Although we are not including the complete derivation in this report, it will help the reader to understand the defining equations below if he keeps in mind the field notations listed in Table 1:

Table 1: Field notation at various system planes

Plane No.	Coordinate	Field	Description
0	ρ_0	$E_0(\rho_0)$	Input field to beam expander
1	ρ_1	$E_1(\rho_1)$	Exit aperture of beam expander
2	ρ_2	$E_2(\rho_2)$	Target plane
$l1$	ρ_{l1}	$E_{l1}(\rho_{l1})$	Virtual focus of secondary mirror
3	ρ_3	$E_3(\rho_3)$	Field received at telescope aperture
4 4 4	ρ_4 ρ_4 ρ_4	$E_4(\rho_4)$ $E_{4'}(\rho_4)$ $D_4(\rho_4)$	Scattered field at detector. LO field at det. Het. det. spatial response function.

In terms of the local oscillator field $E_{4'}$ the collected laser power can be written as

$$R_a P_L = \int d\rho_4 D(\rho_4) |E_{4'}(\rho_4)|^2 \qquad (1)$$

where R_a is the detector responsivity (amps/watt = photon-to-electron conversion factor multiplied by the detector quantum efficiency). The SNR is computed using Eq.(1) for the LO flux in the shot noise expression. The receiver efficiency η is defined for a unit power laser as

$$\eta = \frac{\frac{\lambda^2 z_2^2}{A_0} \int d\rho_2 I_0(\rho_2) |Q(\rho_2)|^2}{\int d\rho_4 D(\rho_4) |E_{4'}(\rho_4)|^2} \qquad (2)$$

where A_0 is the aperture area of the transmitter, z_2 is the distance to the target, $I_0(\rho_2)$ is the target illumination intensity and $|Q(\rho_2)|^2$ is the detector weighted back propagated LO intensity. Eq(2) has been used for determining all the results in this report and η is referred to as the *SNR*.

In all of our calculations we have assumed that the detector size was a circle of 1 Airy disk diameter. In addition all 9.11 μm wavelength calculations where done with a graded reflectivity resonator profile and the other wavelengths were done with a Gaussian resonator profile. All local oscillator fields were assumed to be Gaussian and focused on the detector with an F# similar to the received signal F#.

The results of the analysis are expressed in parametric curves showing the variation of the merit function—the signal-to-noise efficiency—as a function of the various perturbations of the optical system, such as defocus, coma and astigmatism caused by various misalignments. From the parametric data, we derive the optical sensitivities for these factors.

We then derive error budgets and optical tolerances from the parametric sensitivity factors related to the signal-to-noise computations. An assessment of these budgets and tolerances are made with regard to the state of the art, based on a benchmark space-borne optical system, the Hubble Space Telescope. Also, the shorter wavelength system requirements are compared to prior work for the baseline LAWS system. The study concludes by identifying the limiting optical technologies that are challenging to the state of the art and recommending technology-limitation mitigation approaches.

Statement of Work

The technical effort is broken up into three tasks, described in the following.

Task 1.

The variation with wavelength of the overall signal-to-noise ratio of the baseline LAWS system shall be determined for several common optical aberrations and misalignments, including that of the local oscillator. A constant value of backscatter coefficient shall be assumed. Three discrete wavelength values — 1 micrometer, 2 micrometers, and 9.11 micrometers — shall be used. A discussion of the physical optics phenomena causing the computed variations shall be included in the report. The primary output of the task shall be parametric graphs showing how EffSNR varies as focus, tilt, decenter, etc., are varied.

Task 2.

An optical systems error budget for the short wavelength LAWS system shall be constructed, with the optical tolerances apportioned in accordance with the sensitivities defined in task 1. A pointing error budget for the short wavelength case shall also be constructed.

Task 3.

A succinct assessment shall be made of the alignment and other tolerances of task 2 with those achieved on-orbit with the Hubble Space Telescope and any other space optical systems for which there is data. An assessment of the ability of the current technology to achieve the error-budgeted tolerances derived in Task 2 shall be made and documented. Finally, a comparison of a short wavelength LAWS and the baseline CO_2 LAWS system shall be made. A mitigation recommendation shall be made for each technology limitation defined in this study.

Task 1 Results

Discussion and Interpretation

Optical Design for Solid-state Laser

When we learned of the 60-to-1 beam expansion ratio required for a solid-state laser, we were confronted with the choice of accomplishing the beam expansion in one step (as with the CO_2 baseline), or doing it in two steps, perhaps with a 4x beam expander associated with the laser and a 15x beam expansion incorporated in the telescope.

We referred back to the sensitivity analysis performed during the LAWS Phase 2 study[2]. These results indicated that the boresight stability is increasingly sensitive to longitudinal spacing perturbations (i.e. despace) as the beam expansion ratio (or magnification) is increased. In addition, the residual wavefront error due to compensating the Petzval curvature by refocussing would be increased. Extrapolating these earlier results to a beam expansion ratio of 60x showed that the focus (despace) tolerance would be impractical to meet.

Since the beam expansion ratio of 60x appeared to be infeasible, we investigated an optical design that consisted of a 15x telescope and a 4x beam expander associated with the laser itself. We recognized that the wavefront and boresight error budgets would have to be spread over more optical elements, creating somewhat more stringent requirements for each part. As will be shown later in this study, we sub-allocated part of the budget to the telescope and part to the laser beam expander.

---

2 Ref. Pg. 62, Vol. II,GE Astro Space LAWS Final Study Report, Phase II. In this earlier work, the beam expansion ratio was varied: 20x, 33x, and 48x.

The ray traces for the 60x and 15x designs are shown in Figures 1 and 2, respectively. The 60x design is shown here for completeness. However, no additional work was done with this design.

There are two features of the 15x design of Figure 2 that should be noted. It has a larger central obscuration than the 60x design, and the outgoing and receive beams are much closer together. Both of these are the result of the reduced magnification. However, the central obscuration is still only ~0.8% of the aperture area, and the beams do separate before penetrating the primary mirror. The design is feasible although the magnification could not be reduced further before the transmit and receive beams would begin to merge.

Figures 3,4, and 5 show the general effects of spherical aberration, coma and astigmatism, respectively, for the three wavelengths we investigated. The units of the aberrations are micrometers and are expressed as the maximum departure of the aberrated wavefront from an ideal wavefront. The ordinate of the graph is expressed in db, where a db is 10 log (signal-to-noise ratio). Note that the curves start at -3.8 db, corresponding to a signal-to-noise ratio of 0.42, the maximum that can be obtained with a herterodyne system. These curves show that the SNR loss scales roughly with wavelengh (i.e. a given loss will be caused by ~one-tenth as much aberration at 1 μm as would be caused at 9.11 μm) and that the SNR loss falls off quadratically as the aberration is increased.

These curves are somewhat academic in that they do not relate the aberrations to the physical misalignment of an optical system, and that data is what is needed to assess the difficulty of actually manufacturing and aligning a system. The next series of curves illuminates the relationship between the physical misalignments and the SNR.

Figure 6, SNR vs. defocus, shows the actual fall-off in SNR of the 15x beam expander for the three wavelengths considered in the study. There are several things to note in this figure. First, the amount of defocus that is tolerable is smaller as the wavelength is reduced, as expected. Note, however, that the loss in SNR for the 9.11μm case is much less than for the F/1 baseline LAWS[3]. Since the sensitivity of a beam expander to misalignments is generally inversely proportional to the cube of the primary mirror focal ratio, a comparison of this curve with the referenced curve illustrates very graphically the relief from tight alignment tolerances that a slower primary mirror focal ratio can buy. (Of course, a slower primary mirror requires more overall length.)

---

[3]Refer to Figure 3.2-3, Page 52, Volume II of the Phase II LAWS Final Report. For a point of comparison, note that the loss due to 10 μm of defocus in that figure converts to about -0.5 db, while the loss for the new F/2, 60 cm design is negligible (at the same wavelength).

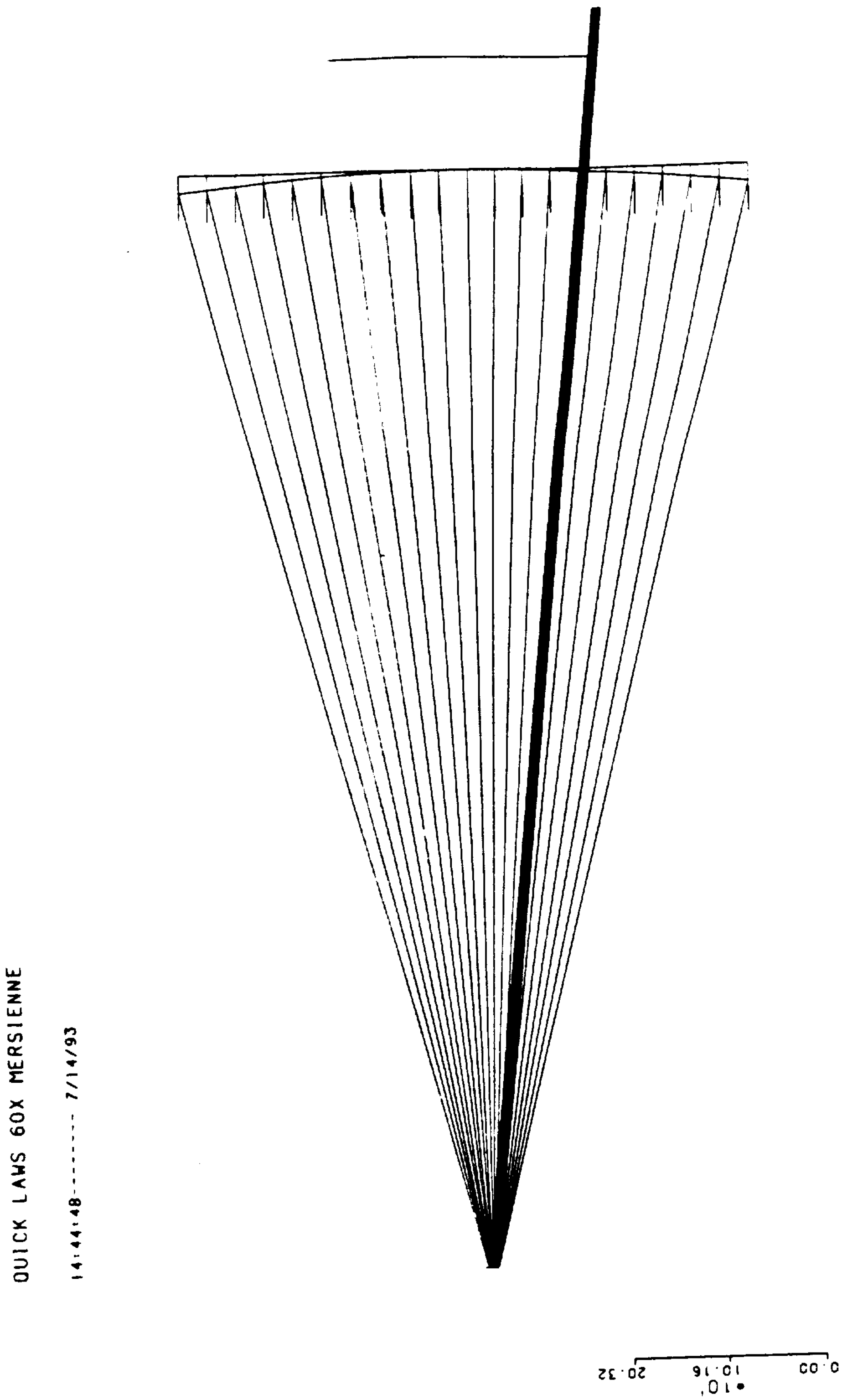

Figure 1. 60x Beam Expander.

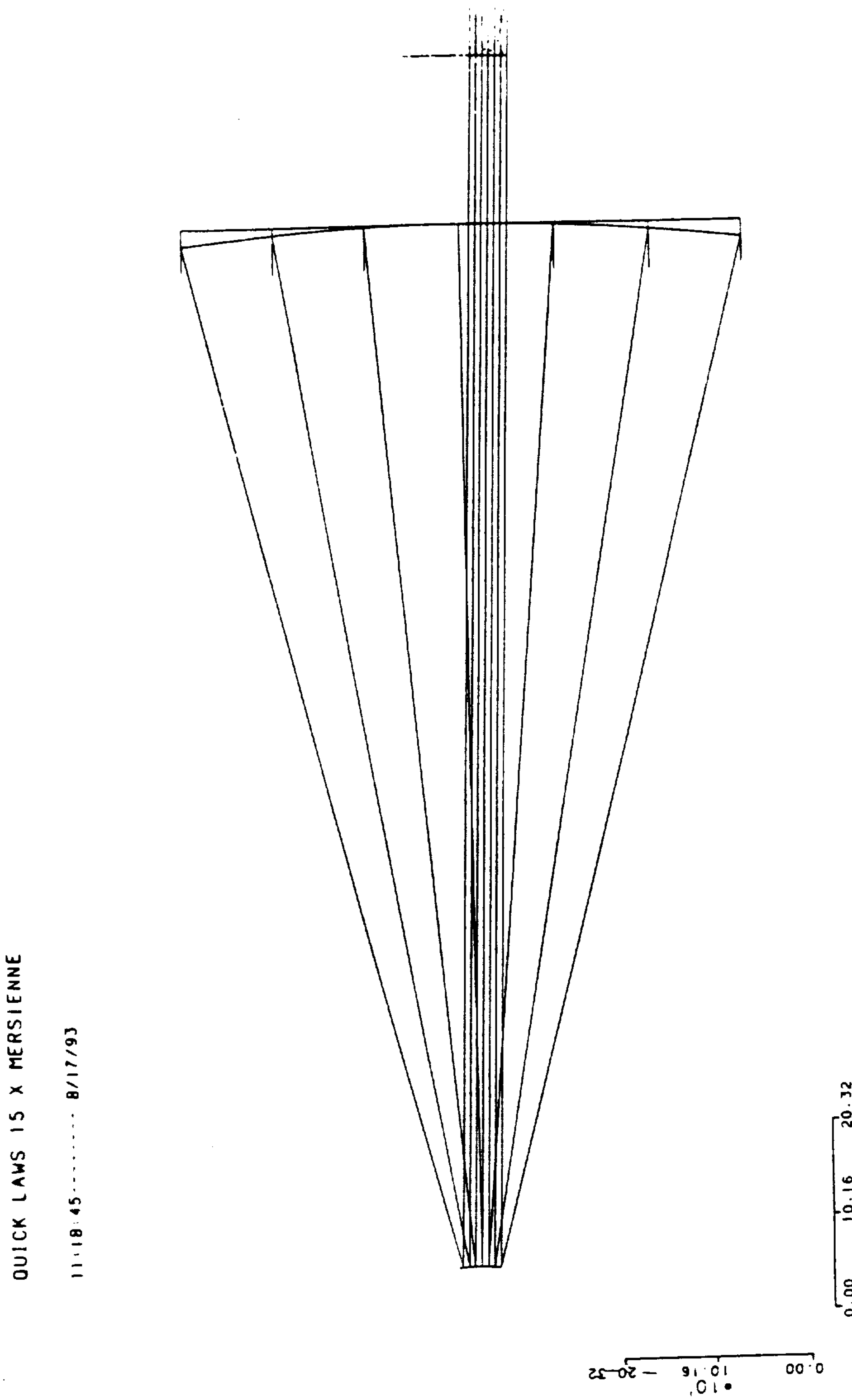

Figure 2. 15x Beam Expander.

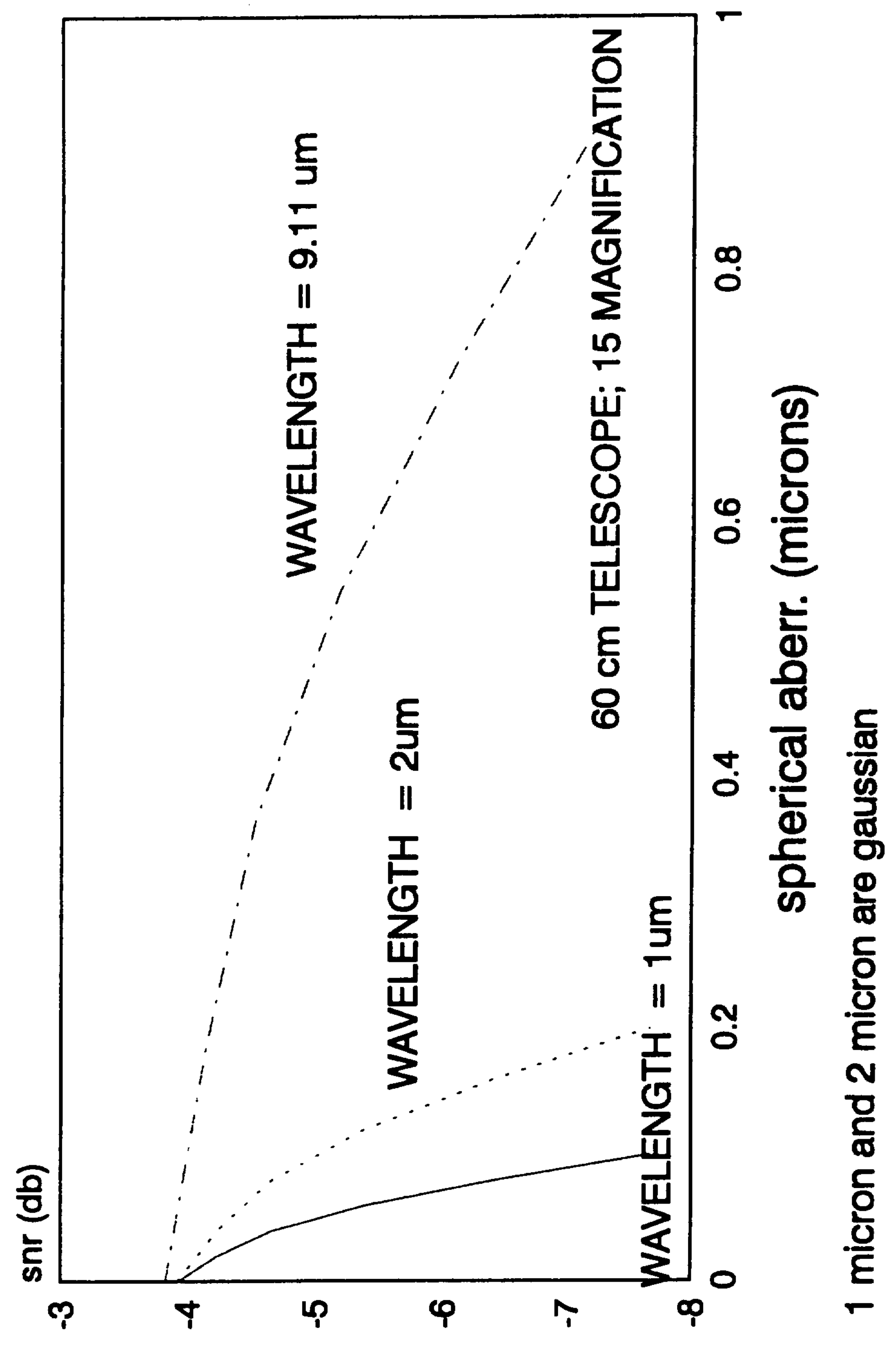

Figure 3. SNR vs. Spherical.

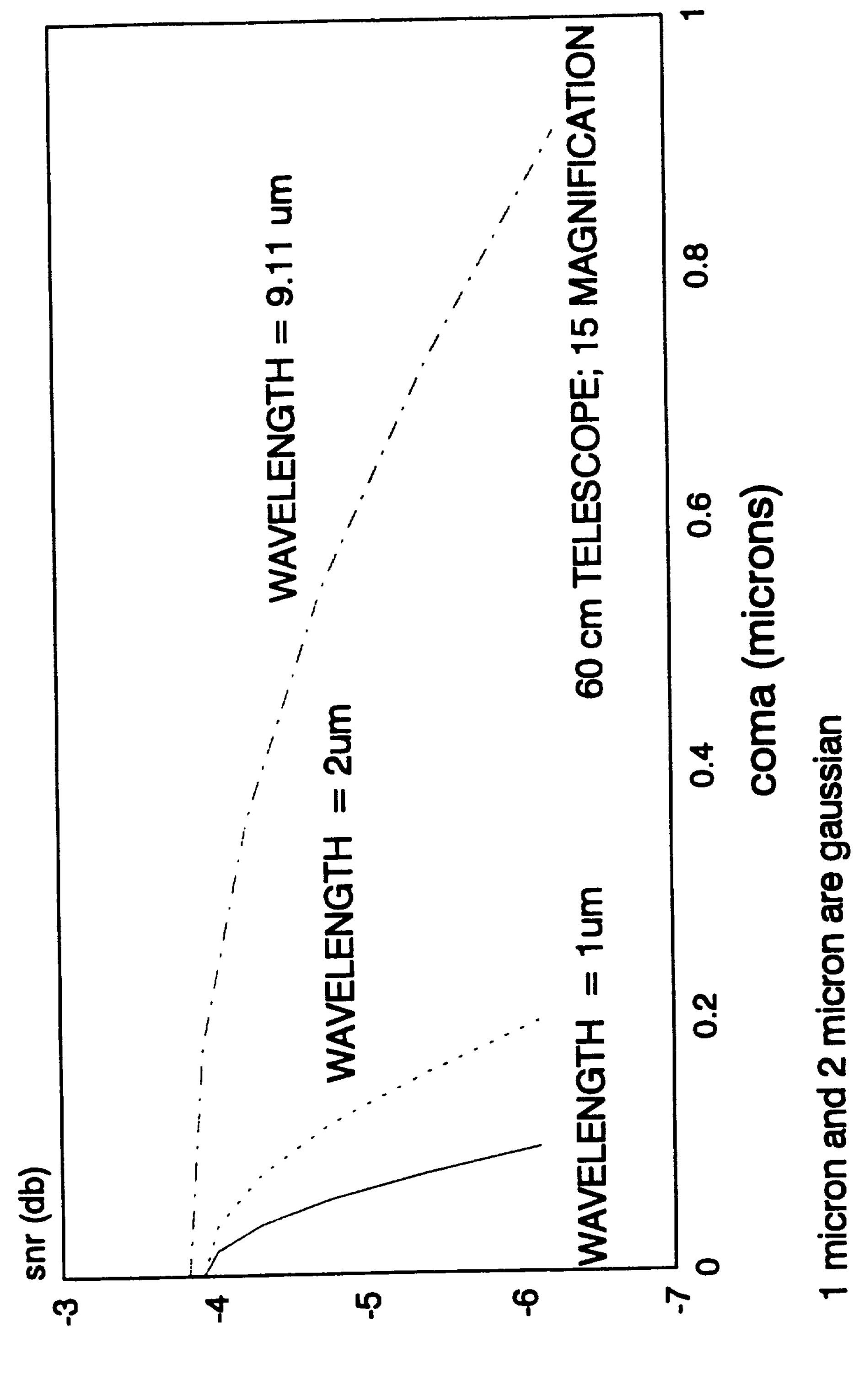

Figure 4. SNR vs. Coma.

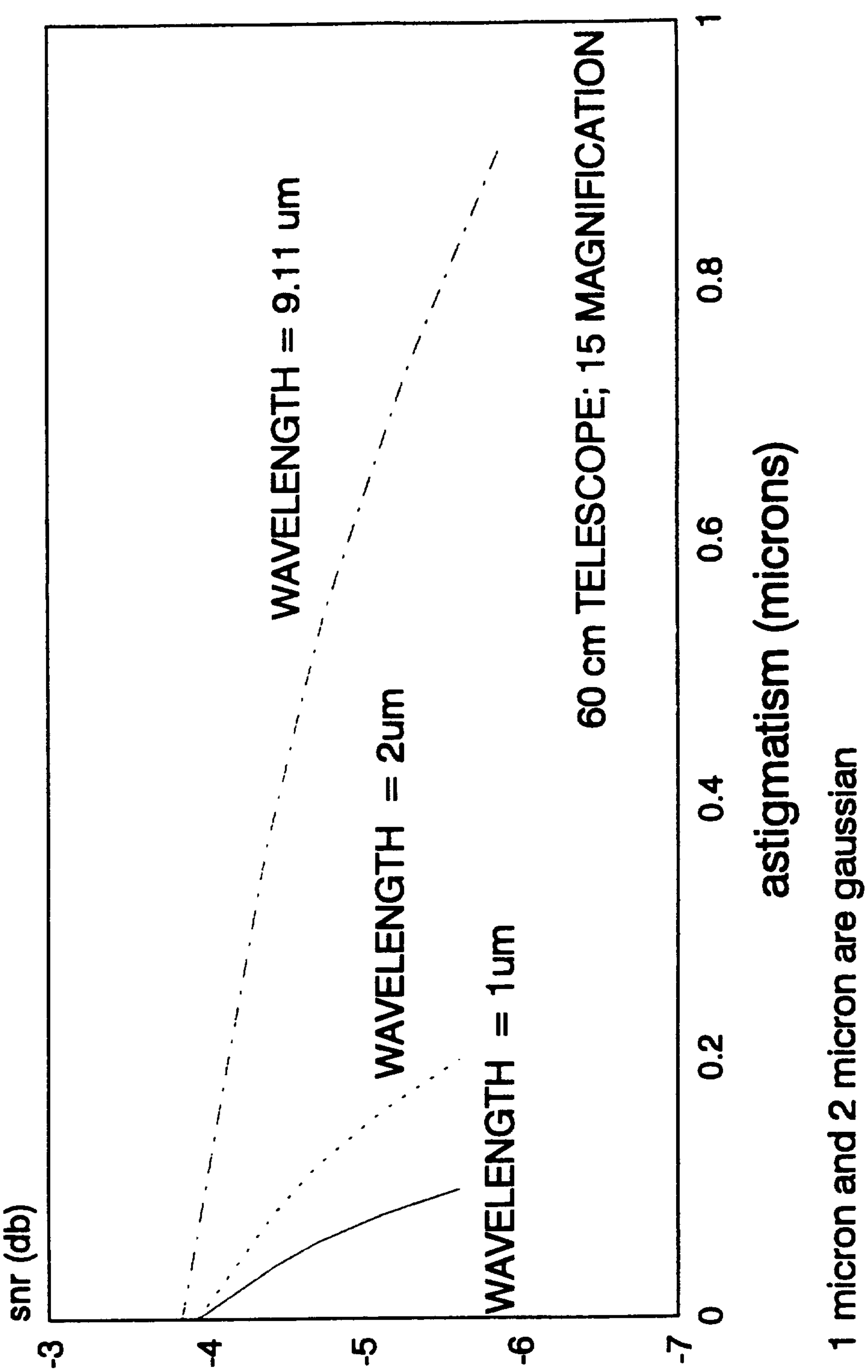

Figure 5. SNR vs. Astigmatism.

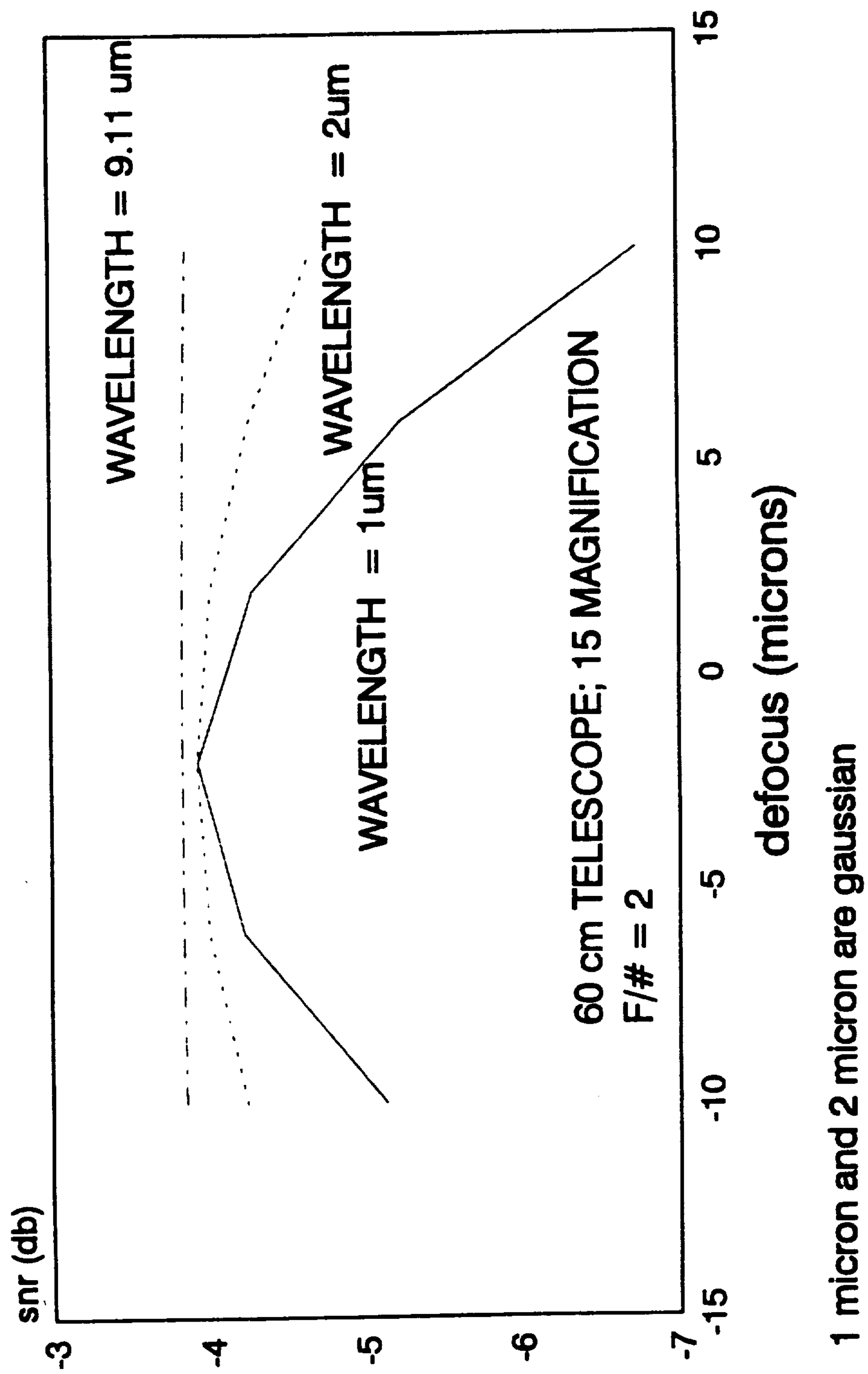

Figure 6. SNR vs. Defocus.

Third, note that that the SNR loss is not proportional to wavelength. At 5 μm of defocus, a loss of ~ 0.8 db occurs in going from 2μm to 1μm, rather than the expected 3 db loss if the loss was a linear function of wavelength. The loss in going from 9.11μm to 2 μm is only ~0.2db (about 5%). This apparantly contradictory result can be understood through reference to the theory of diffraction[4]. The reference shows that the intensity in the neighborhood of focus varies in accordance with the sinc function (referring specifically to Eqn. 26 of the reference). The argument of the sinc function is inversely proportional to the wavelength (and the system focal length), and also contains the diameter of the aperture (squared), and the amount of defocus. In our analysis, only the wavelength and focal length can vary. Since we are re-normalizing to maintain a detector size equal to the Airy disk diameter, we are in effect partially compensating the change in wavelength through this mechanism. Therefore, we have two effects that mitigate the change in wavelength: the non-linearity of the sinc function and the variation in the system effective focal length. The shape of the curves is indicatative of the central portion of the sinc function. The second effect is real and important, since the physical detector size is determined by manufacturing considerations, while the effective focal length of the system can be made almost any value, set only by the focal length of the final lens in the receiver.

Figure 7 shows the variation of SNR as a function of decenter of the secondary mirror. In this case, the loss of SNR is proportional to the wavelength for a given amount of decenter. This is expected since the basic variable in the theory of diffraction is $2\pi/\lambda$, and there are no compensating variables in the case of an unsymetric aberration, such as the coma caused by the secondary mirror decenter misalignment.

In the Phase 2 study, we investigated the effect of a tilt misalignment of the beam expander optics and found that there was very little effect on SNR. In fact, if the the tilt alignment does not change during the pulse echo time, there will be no effect (except if there is also a tilt misalignment of the LO beam, a case adequately covered in the literature). Because if this prior knowledge and the limited scope of this study, we did not repeat this part of the investigation.

Sensitivities

The 15x optical design ray trace was perturbed by making relative unit changes in decentration, tilt and rotation of the optical elements. The resulting changes in the Zernicke polynomials (representing the wavefront error) and the wavefront tilt (representing boresight errors) were tabulated for use in the heterodyne signal-to-noise efficiency calculation.

---

[4] Born and Wolf, *Principles of Optics*, Third Edition, Pages 440-441

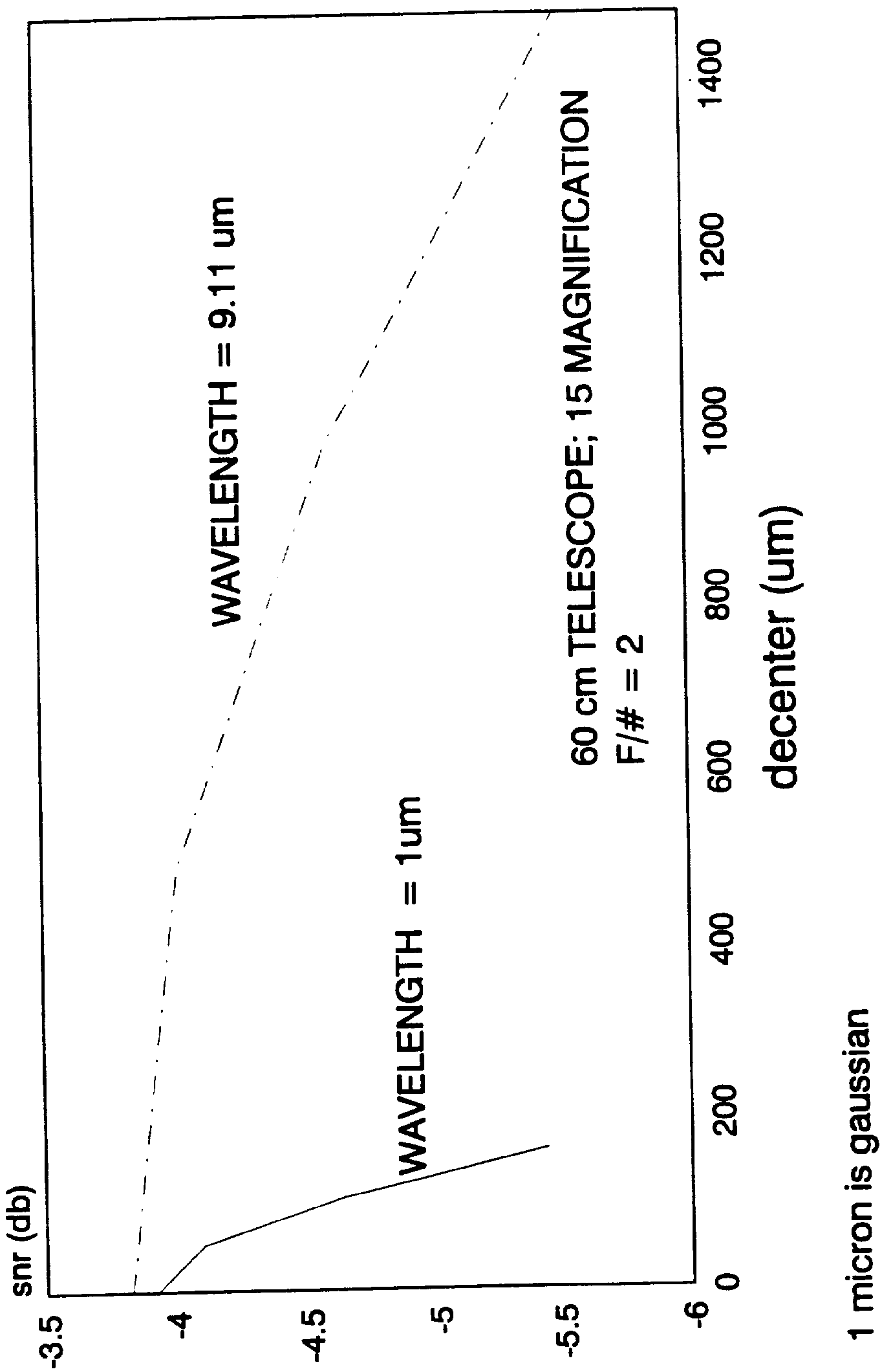

Figure 7. SNR vs. Decenter.

The basic ray trace data and the effects of the unit perturbations are included in this report as Appendix 1.

For the purposes of this study, the laser beam is assumed to have a Gaussian profile before truncation. (In the referenced study, the effect of a typical non-Gaussian beam profile was shown to cause ~5% loss in SNR.) The sensitivity information in this data was incorporated into the error budgets that follow.

Task 2 Results

Wavefront Error Budgets

We shall follow the same error budgeting philosophy as in the Phase 2 study Error Budget Report[5] in evaluating the impact of the wavelength change. As shown in Figure 4-1, Page 11 of that report, the heterodyne efficiency was allocated an absolute value of 0.23 and was distributed among laser wavefront, aberrations, beam truncation, laser beam tilt and pointing error. The top of this efficiency budget tree showed an overall efficiency value of 0.08. Although not indicated in the report, the error contribution for aberrations was a multiplicative factor of 0.9, corresponding to a wavefront error of $\lambda/20$ rms. For reference, the optial wavefront error budget that was prepared for the Phase 2 study in support of the error budget report is reproduced here as Figure 8. Since the optical quality affects both the outgoing and the receive beam, it is important to maintain an equally high optical quality for the solid-state laser system.

As an aid to understanding the error budget charts, note that all the quantities that are left-indented are the root-mean-squared fractions of a wavelength that the actual optical wavefront is permitted to depart from an ideal wavefront. The right-indented figures are the applicable engineering or metrology tolerances that produce the wavefront errors. The tolerances are related to the wavefront errors by the sensitivities computed in the MEXP runs (listed in the Appendix). In each branch of the error tree, the individual wavefront errors are root-sum-squared to yield the quantities in the boxed entries, and finally, the boxed quanitities are root-sum-squared to yield the allocated quantity at the head of the error budget tree. Provided the margin is posititive, it is used in the calculation of the wavefront error (or top box on the chart). This convention is consistent with that used in the HST error budgets.

---

[5]GE Astro Space Phase 2 Data Requirement Document DR-13, Error Budget Report, June 10, 1993

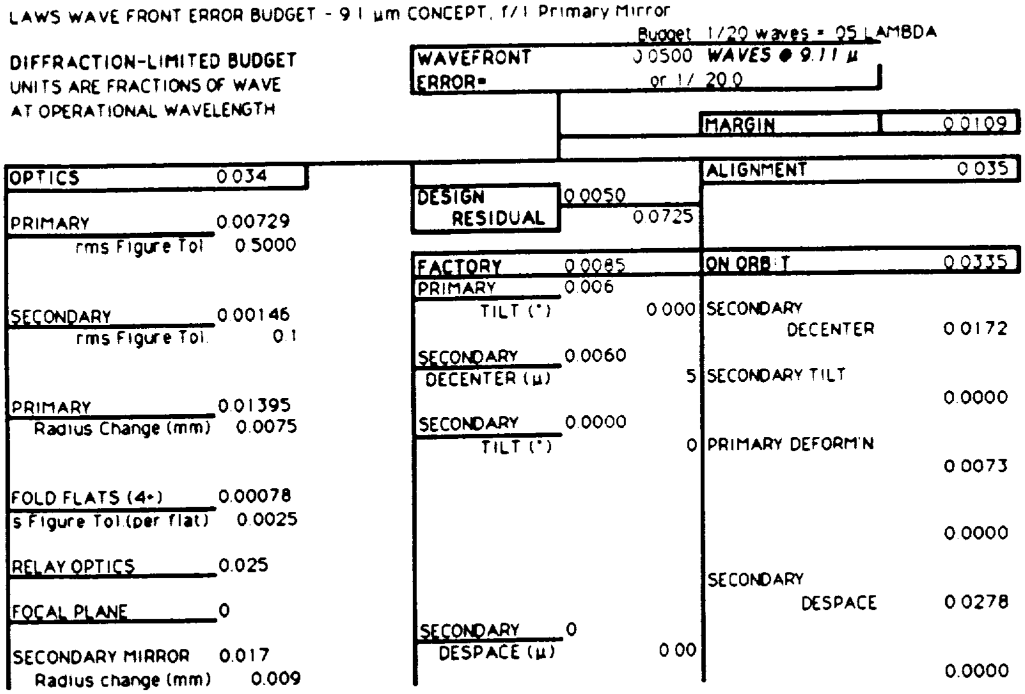

Figure 8- Baseline (1.5µm, CO_2) wavefront error budget.

The worst-case (i.e. for a wavelength of 1 µm) sub allocation of wavefront errors is shown in Figure 9 below. The new design is more forgiving of some errors, but the reduced wavelength requires some tightening of tolerances. An attempt was made to maintain the three top levels for the optics, alignment and margin about the same as for the baseline system. It should be appreciated that there is a nearly infinite combination of error allocations that could be made. However, some knowledge of manufacturability went into the allocations shown.

Tolerances on the primary and secondary mirror figure quality had to be tightened up. The $\lambda/10$ figure tolerance (λ= 6328Å) for the primary mirror and the $\lambda/50$ figure tolerance for the secondary are within the state of the art. The margin was increased to allow for the errors that will be contributed by the 4x expander needed for the laser. (This expander was not designed and therefore no error budget was created).

We shall evaluate these tolerances relative to the benchmark optical system—the Hubble Space Telescope—in the final section of this report.

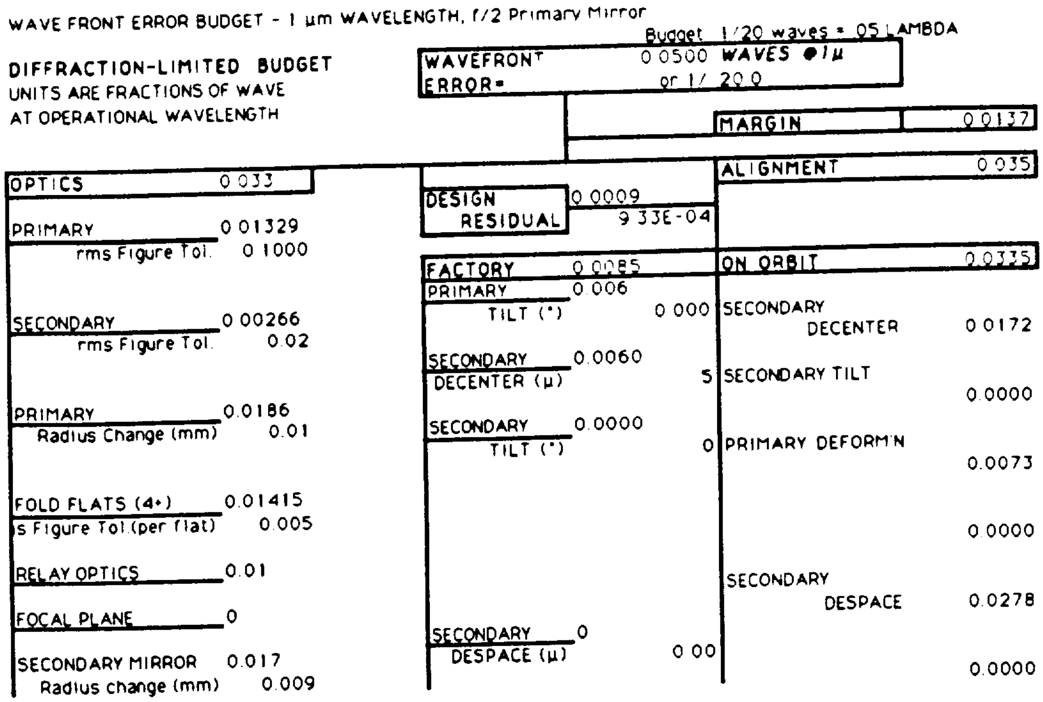

Figure 9 Wavefront error allocation for f/2, 1µm optical system.

Pointing Error Budgets

We will allocate the pointing errors in the same proportions as was done in Data Requirement DR-8, Section 4.4.1.7 of the Phase 2 documentation. Pg. 42. For reference, the CO_2 baseline error budget is reproduced here as Figure 10.

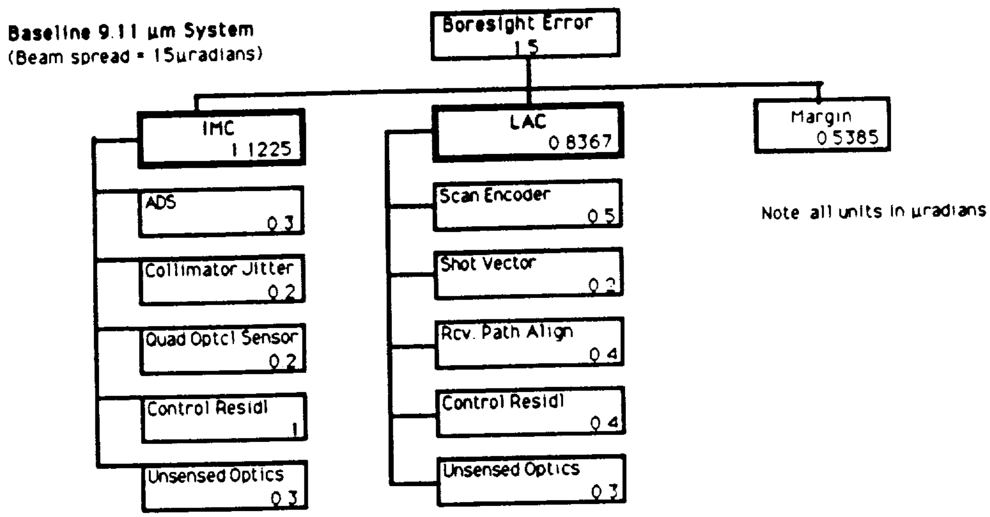

Figure 10. Overall baseline (CO_2) Pointing Error Budget, in format of Phase 2 DR-8.

The back-up for this overall budget showing the realtionship between the allocated errors and the physical tolerances for various parts of the system is shown as Figure 11.

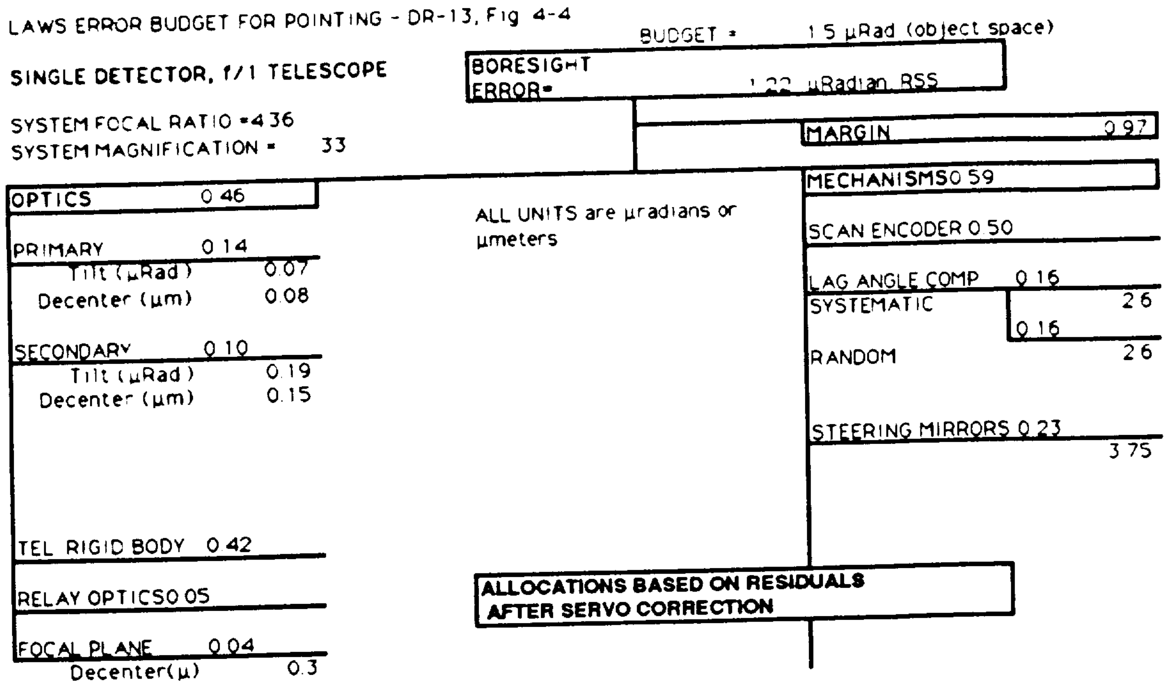

Figure 11. Detailed baseline (CO_2) error budget showing relationship between allocated error and physical tolerances.

The equivalent top-level error budget in the format of DR-13 reduced aperture Quick-LAWS, the equalivalent pointing error budget is shown in Figure 12:

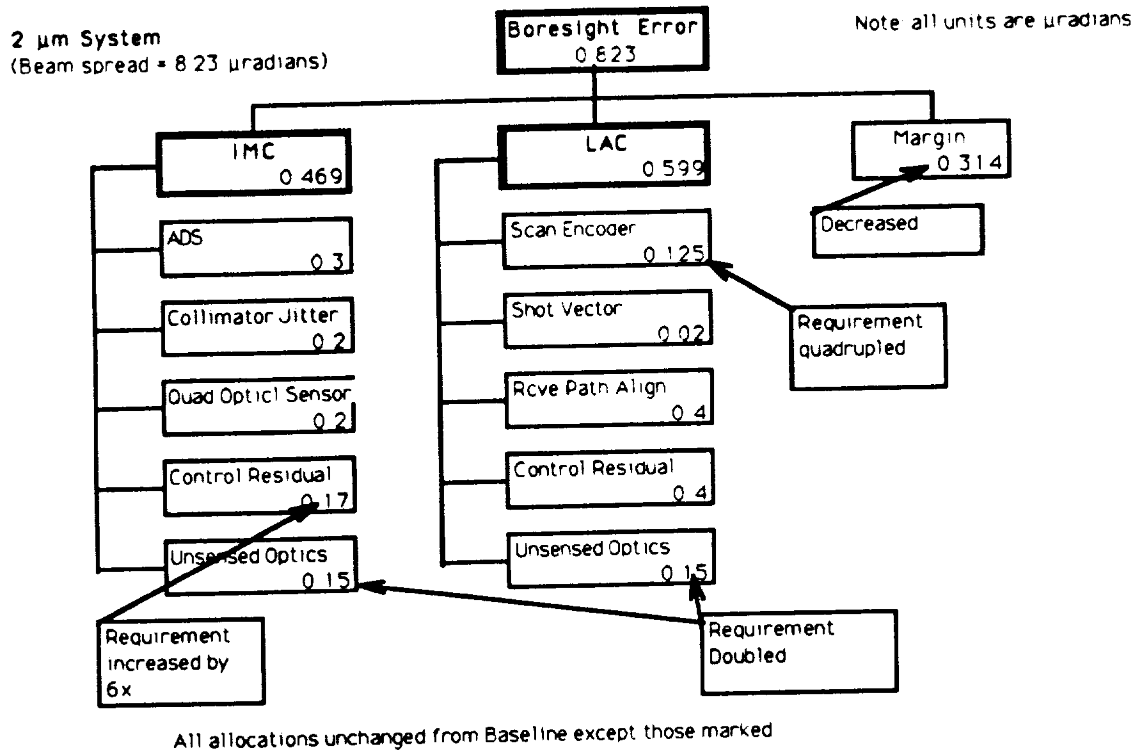

Figure 12. Pointing error budget for 60cm, 2µm system.

The detailed back up for the error allocation of Figure 12 is shown below in Figure 13.

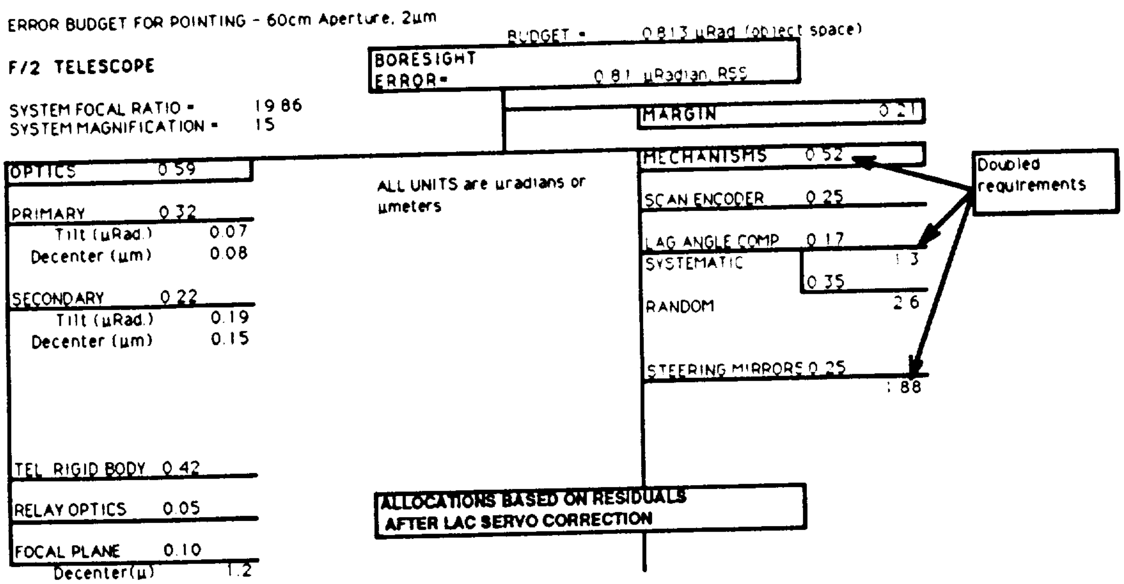

Figure 13. Detailed tolerancing allocation for 2μm 60 cm system.

Task 3 Results

Comparison with baseline space optical system(s)

The benchmark optical system that we will using to determine whether or not the error budgets and optical/structural tolerances are within the state of the art is the Hubble Space Telescope (HST). Orbital operations of the HST have shown that the Fine Guidance Sensor subsystem has met its contractual requirements, both for jitter and long-term stability. Therefore, the error budgets and performance predictions that were made during the design of the telescope can be used with confidence.

The primary references that were used in this study are: 1) Report ST 1464-78B, Contract NAS 8-32700, "OTA Image Stability, Pointing Error Budget Report", Rev. B, 21 September 1984, and 2) Report ST 0694-80C (SE-03J), Contract NAS 8-32700, "FGS 24-Hour Image Stability Pointing Error Budget", Rev. C, March 1986. Where necessary, figures and text from these reports are reproduced here to assist the reader.

The comparison between the HST and a future Doppler lidar must be done with a great deal of care. A number of caveats must also be kept in mind. However, the chief value of the comparison is to indicate the main areas of difficulty in tolerancing a lidar system.

Some of the caveats include the differences in the missions and the time scales involved (many hours for an exposure in HST; a few milliseconds for LAWS), the relative sizes of the two instruments (a ratio of four in aperture size), and the shorter (UV and visible) wavelengths for the HST mission.

On the other hand, technology has moved ahead since the HST was designed in the mid-'70's, and somewhat better performance can reasonably be expected with today's materials and design techniques.

Please refer now to Figures 14 and 15, reproduced from ST-1464-78B, and in particular, the optical error budget, shown in detail in Figure 15. As we learned earlier in our study, the most sensitive tolerance parameter is the relative decenter of the primary and secondary mirrors. In the figure, note that the budget is given as 10μm (random—R) and ± 10μm for the slowly varying (—S), while the predicted values are 0.3μm and 3.5μm, respectively. These values compare with our allocated decenter tolerance of 0.15 μm for the 2μm wavelength system. If we can responsibly dismiss the slowly varying (10μm and 3.5μm) decenter

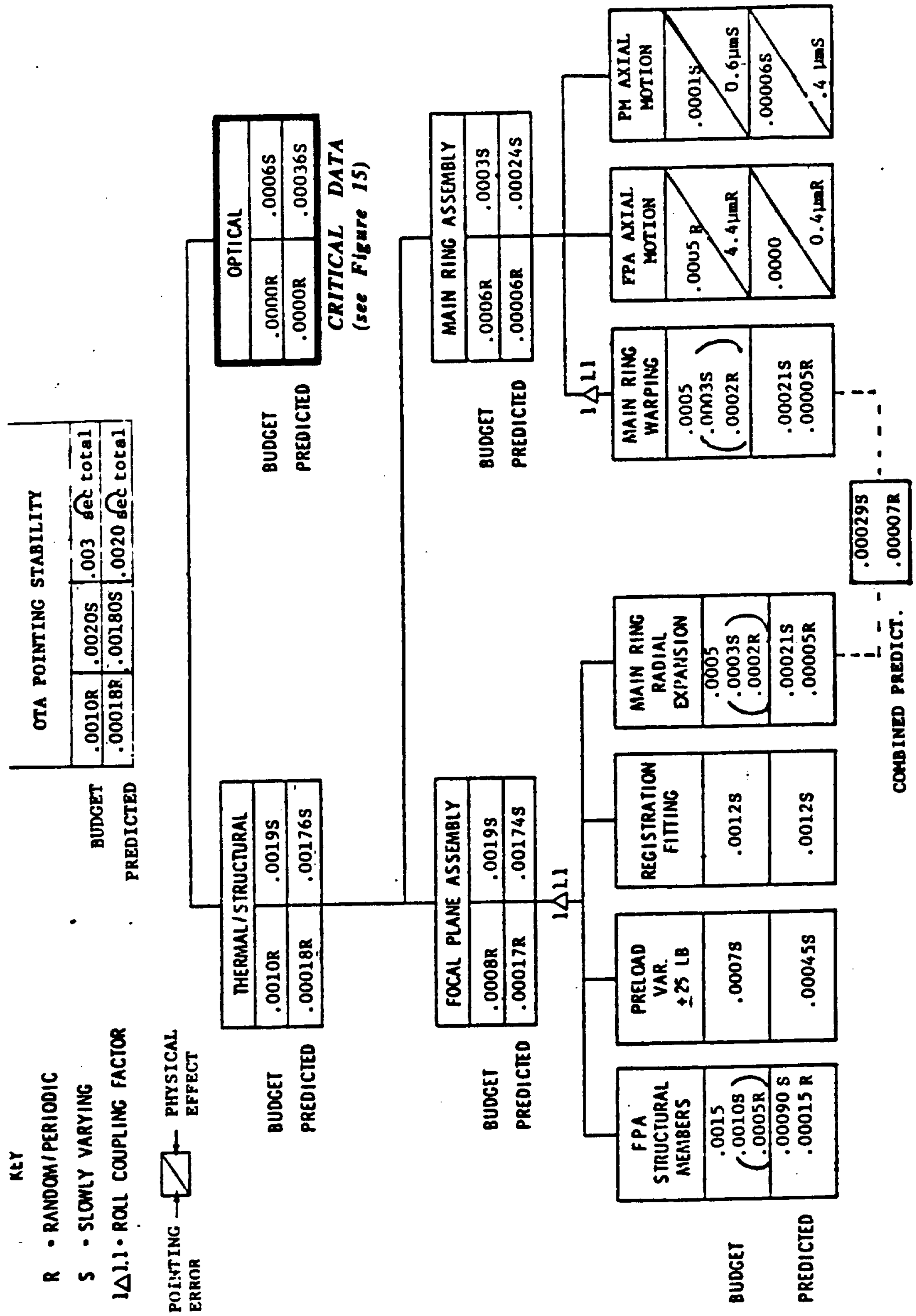

Figure 14. HST Error Budget.

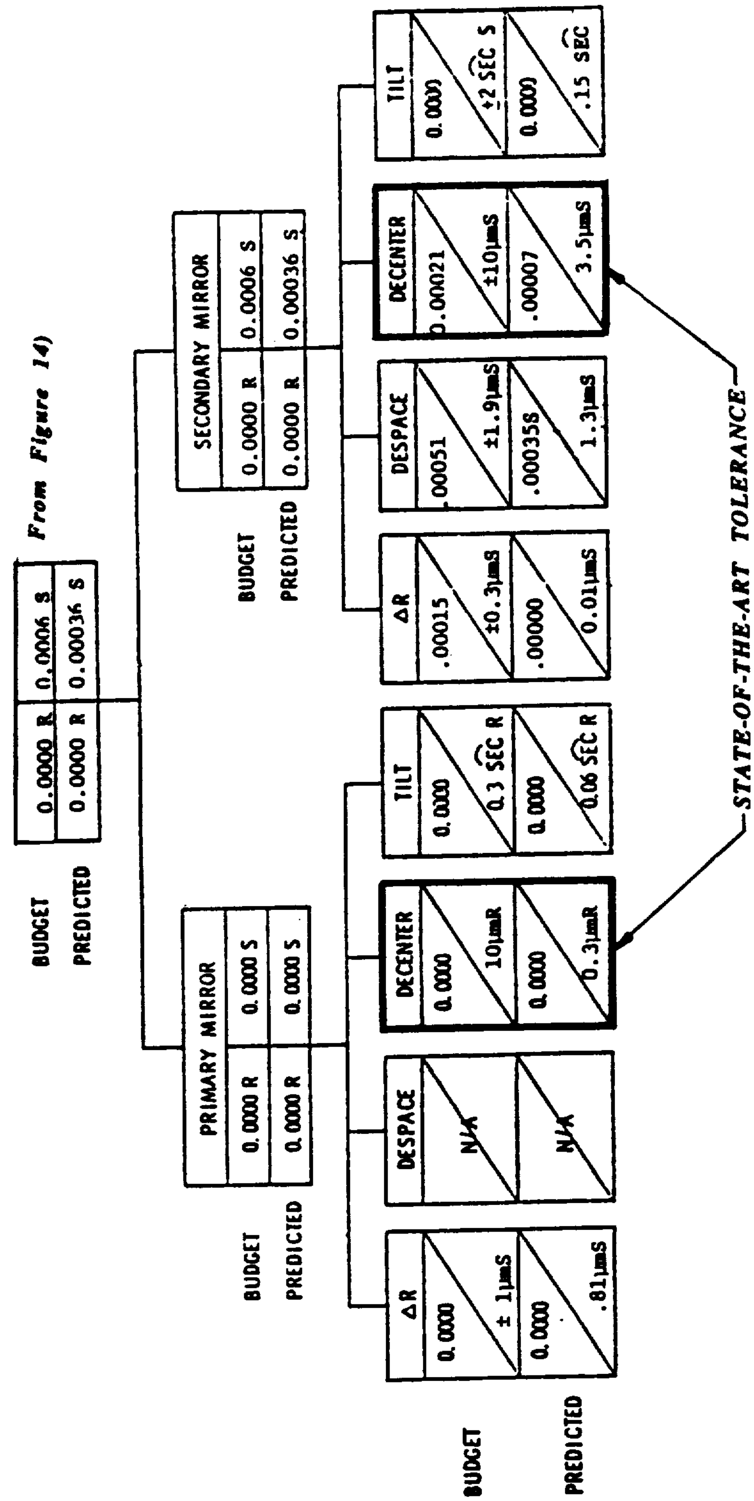

Figure 15. HST Error Budget (Page 2).

tolerances on the basis of having a negligible effect on SNR (ref. Figure 7), and assume that tighter decenter tolerances could he held in this smaller lidar system, than a tolerance that is twice as tight as the HST tolerance may be feasible. Much more study and design effort is necessary before a final decision could be made regarding the feasibility of achieving the required tolerances.

Comparison with baseline CO_2 LAWS system

Conclusions and Recommendations

Our study has revealed some positive, unexpected results. We learned that the scaled-down system with a slower primary mirror is somewhat forgiving of the greatly increased performance requirements of a shorter operational wavelength. In addition, we learned that there are techniques for compensating for the effects of defocus, albeit at the expense of increased back focal length of the receive part of the system (roughly in the ratio of the CO_2 wavelength to the new laser wavelength).

However, the overall pointing stability requirement for a high performance heterodyne lidar system is probably a stretch for a 2µm system, and beyond the state-of-the-art for a 1µm laser. Note that the pointing accuracy requirement for a 2 µm laser is increased by an overall factor of 1.8 (increased by 4.5 for the smaller wavelength, but decreased by a factor of 2.5 for the 60cm aperture), while the pointing requirement for a 1µm laser is 3.6 times as difficult as the 1.5m baseline LAWS system. We did not attempt to tolerance the 1µm system since the necessary tolerance assignment could not be taken seriously.

This small study was a rather cursory look at a new optical design and error budget/tolerances allocations for a space-borne solid-state lidar system. Its basic premise was that performance similar to the baseline CO_2 LAWS system was needed. If NASA is interested in pursuing the subject for a solid-state laser system, we offer the following recommendations:

- Extend the optical design to include the 4x beam expander for the solid-state laser, and add a sensitivity and error budget for these elements. (This work was not included in the present study due to its limited scope.)
- Perform a design and analysis of the complete receive path optical train, incorporating the LO characteristics for a solid-stste laser
- Establish an overall performance requirement (i.e. SNR) within specific cost and physical interface parameters

- Re-visit the Phase 1/2 study system-level trades and preliminary design studies, specifically in the areas of alignment and pointing stability

- Fund a bread-board program to determine experimentally the achievable performance of a lag angle compensation system.

Appendix 1 Ray Trace Data

$ LOGOFF
BOLAND logged out at 14-JUL-1993 17:45:21.45

WAVELENGTH 0.632800 0.486133 0.656272 PHI 0.000000E+00

NO.	SURFACE TYPE	TILT TYPE	DIFFRACT TYPE	RADIUS	THICKNESS	MD-INDEX	HI-INDEX	LO-INDEX	ABBE NO.	GLASS NAME	CLEAR APERT	OUTER BOUND	INNER BOUND
0	ENTRANCE PUPIL				0.0000	1.000000	1.000000	1.000000					
1	SPHERE	NORMAL		INFINITE	0.0000	1.000000	1.000000	1.000000	0.00	AIR	600.00	0.00	0.00
2	ASPHERE			-2400.0000	-1120.0000	-1.000000	-1.000000	-1.000000	0.00	-AIR	610.07	0.00	0.00
3	ASPHERE			-160.0000	1300.0000	1.000000	1.000000	1.000000	0.00	AIR	16.15	0.00	0.00
4	SPHERE			INFINITE	0.0000	1.000000	1.000000	1.000000	0.00	AIR	241.20	0.00	0.00
5	SPHERE			INFINITE	0.0000	1.000000	1.000000	1.000000	0.00	AIR	241.20	0.00	0.00

TABLE OF DECENTRATIONS, TILTS AND ROTATIONS

NO.	TYPE	X-DEC.	Y-DEC.	Z-DEC.	(Y-TILT) THETA Z	(Z-TILT) THETA Y	THETA X
1	1		0.000000E+00	0.000000E+00	1.000000E-01	0.000000E+00	0.000000E+00

SURFACE TYPE 2 ASPHERIC COEFFICIENTS

NO.	Epsilon (CC+1.0)	C'	D'	E'	F'
2	0.000000E+00	0.000000E+00	0.000000E+00	0.000000E+00	0.000000E+00
3	0.000000E+00	0.000000E+00	0.000000E+00	0.000000E+00	0.000000E+00

FIRST ORDER PARAMETERS ON Y-MERIDIONAL PLANE

MEASURED FROM FIRST SURFACE / MEASURED FROM LAST SURFACE

OBJECT DSTNCE	ENTR.PUP.DIST	FRST.PPAL.PNT	AFOCAL-U	SCND.PPAL.PNT	EXT.PUP.DSTNC	IMAGE DISTNCE
INF	0.000000	INF	0.000000	INF	-1374.666667	INF
OBJECT HEIGHT	**ENTR.PUP.DIAM**	**OBJT.SPCE.FNO**	**INF.OBJCT.FNO**	**IMGE.SPCE.FNO**	**EXT.PUPL.DIAM**	**IMAGE HEIGHT**
INF	600.000000	INF	**************	INF	40.000000	INF
MAGNIFICATION	**SEMIANG.FIELD**	**BACK VTX.DIST**	**BARREL LENGTH**	**FRNT.VTX.DIST**	**SEMIANG.FIELD**	**DEMAGNIFICATION**
0.066667	0.100000	INF	160.000000	INF	1.500000	15.000003
APT.STOP DIAM	**APT.STOP DIST**	**FROM SRFCE.NO**	*************	**FLD.STOP DIAM**	**FLD.STOP DIST**	**FROM SRFCE.NO**
600.000000	0.000000	0	***AFOCAL****	INF	INF	4

MCASE	FNO/SIZE	AFOCAL CODE	TARGET OBJ DIST	TARGET F.L.	OBJ.CURV	BASE COLOR	Y-YBAR	OBJ/IMG
2	1	1	0.00000+00	1.00000+00	0.00000+00	3	0	-9

REAL ENTR. PUPIL CODES 0 0

ORIGINAL PAGE IS
OF POOR QUALITY

Appendix 2 Parametric Curves for Scaled Baseline System

SNR VS DEFOCUS

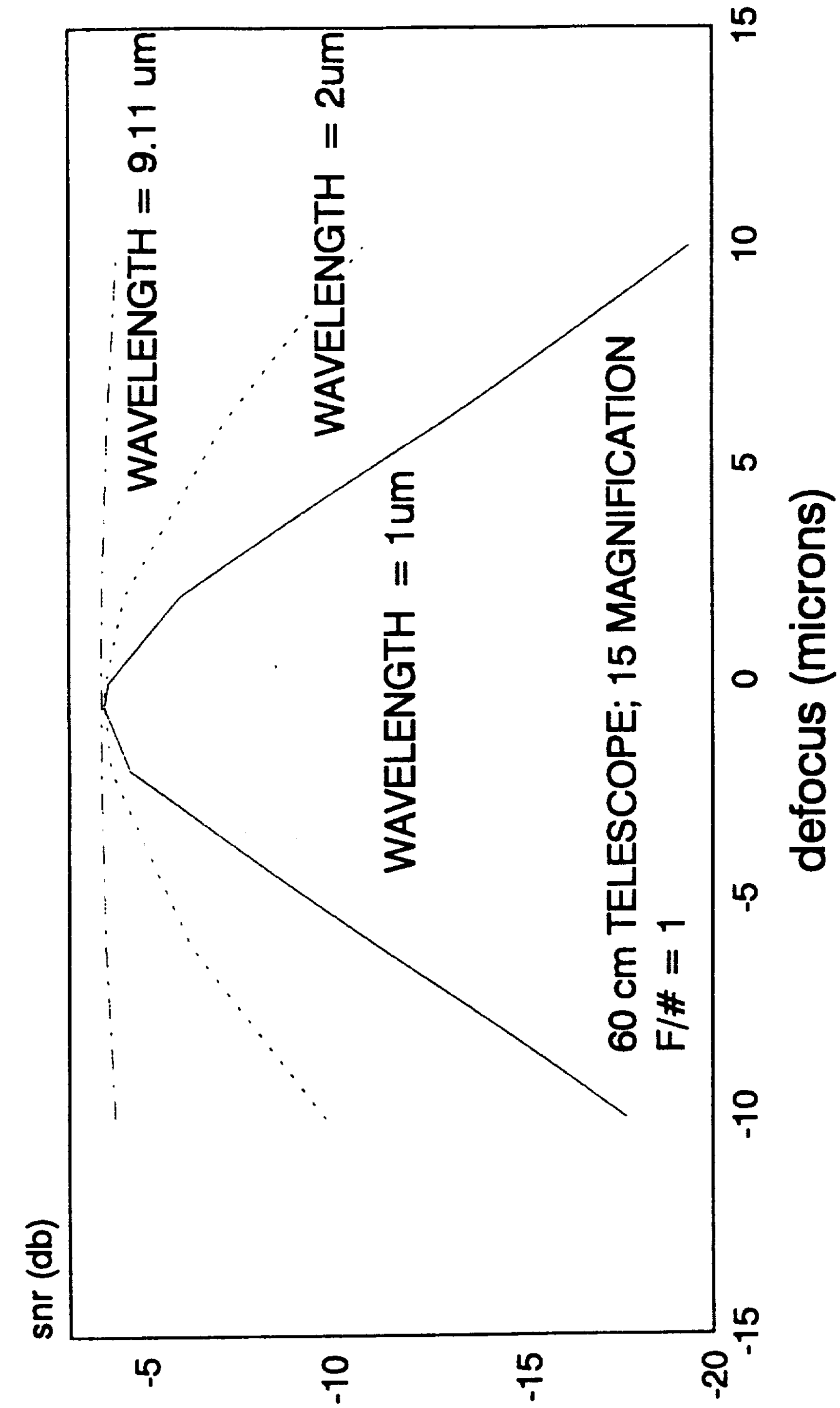

1 micron and 2 micron are gaussian

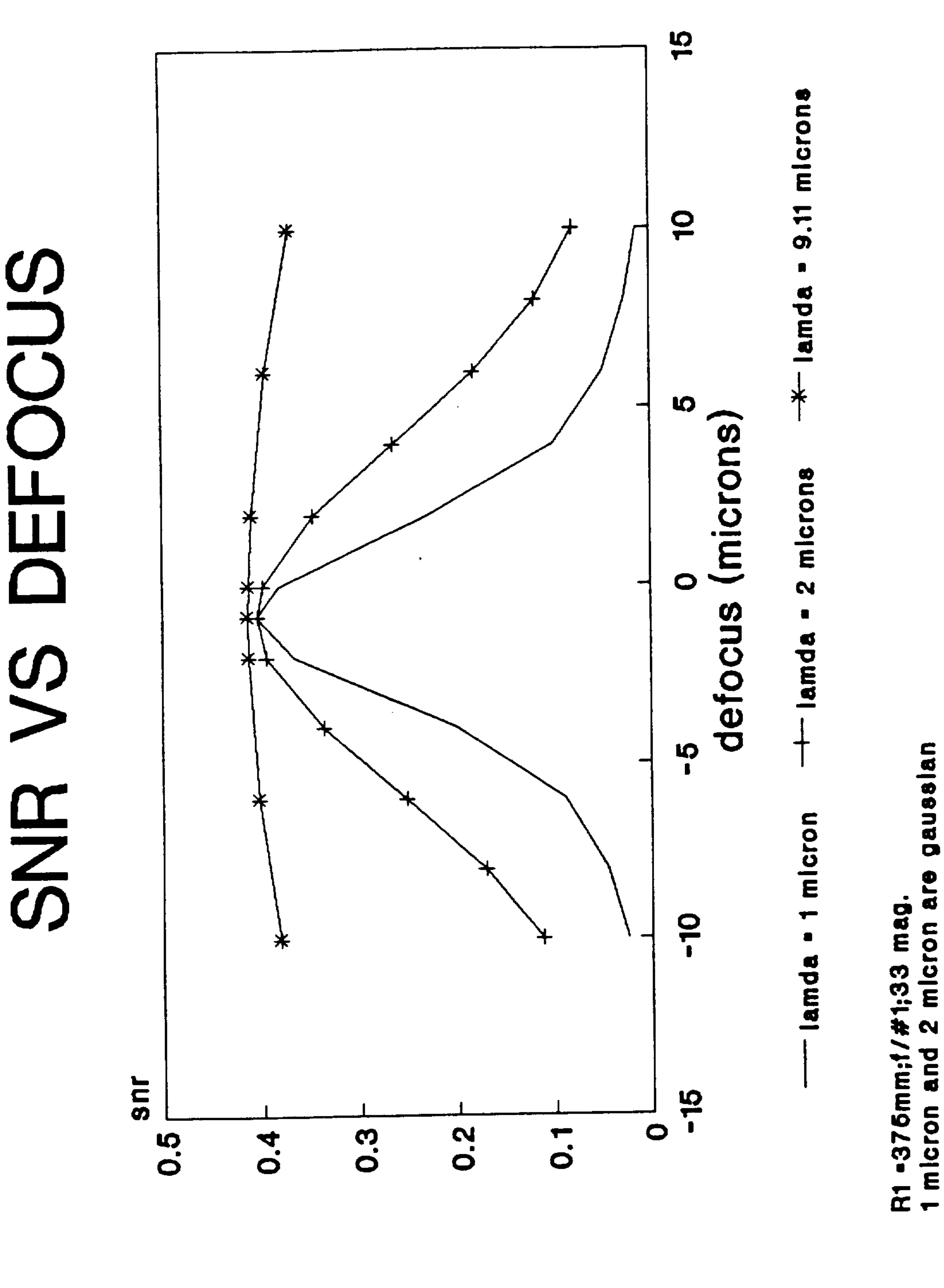
SNR VS DEFOCUS
snr
0.5
0.4
0.3
0.2
0.1
0
-15
-10
-5
0
5
10
15
defocus (microns)
lamda = 1 micron
lamda = 2 microns
lamda = 9.11 microns
R1 =376mm;f/#1;33 mag.
1 micron and 2 micron are gaussian

HUGHES

Hughes Danbury Optical Systems, Inc.
a subsidiary

NASA
National Aeronautics and Space Administration

Report Documentation Page

1. Report No.	2. Government Accession No.	3. Recipient's Catalog No.
4. Title and Subtitle IMPACT OF SHORTER WAVELENGTHS ON OPTICAL QUALITY FOR LAWS		5. Report Date September 1993
		6. Performing Organization Code
7. Author(s) Alan B. Wissinger		8. Performing Organization Report No. PR D15-0018
		10. Work Unit No.
9. Performing Organization Name and Address Hughes Danbury Optical Systems, Inc. (HDOS) Danbury, CT 06810-7589		11. Contract or Grant No. H-207520
12. Sponsoring Agency Name and Address National Aeronautics and Space Administration Washington, D.C. 20546-0001 Marshall Space Flight Center		13. Type of Report and Period Covered Final
		14. Sponsoring Agency Code

15. Supplementary Notes

Monitor of Contract: Dr. R. J. Koczor

16. Abstract

This study explores parametrically as a function of wavelength the degrading effects of several common optical aberrations (defocus, astigmatism, wavefront tilts, etc.), using the heterodyne mixing efficiency factor as the merit function.

A 60 cm diameter aperture beam expander with an expansion ratio of 15:1 and a primary mirror focal ratio of f/2 was designed for the study. An HDOS copyrighted analysis program determined the value of merit function for various optical misalignments. With sensitivities provided by the analysis, preliminary error budget and tolerance allocations were made for potential optical wavefront errors and boresight errors during laser shot transit time. These were compared with the baseline 1.5 m CO_2 LAWS and the optical fabrication state of the art (SOA) as characterized by the Hubble Space Telescope. Reducing wavelength and changing optical design resulted in optical quality tolerances within the SOA both at 2 and 1 µm. However, advanced sensing and control devices would be necessary to maintain on-orbit alignment. Optical tolerance for maintaining boresight stability would have to be tightened by a factory of 1.8 for a 2 µm system and by 3.6 for a 1 µm system relative to the baseline CO_2 LAWS. Available SOA components could be used for operation at 2 µm but operation at 1 µm does not appear feasible.

17. Key Words (Suggested by Author(s)) Laser Atmospheric Wind Sounder Doppler LIDAR Optical Quality Heterodyne Efficiency	18. Distribution Statement Unclassified - Unlimited Copyright © Hughes Danbury Optical Systems, Inc. 1993 Subject Category: Physics/Optics

19. Security Classification (of this report)	20. Security Classification (of this page)	21. No. of pages	22. Price
UNCLASSIFIED	UNCLASSIFIED	32	

HQ 1680A